Scattered-Light Noise for LIGO
(LIGO Technical Report LIGO-T950132-00-R)

Eanna E. Flanagan and Kip S. Thorne
Enrico Fermi Laboratory, University of Chicago, Chicago IL 60637;
and Theoretical Astrophysics, California Institute of Technology, Pasadena, CA 91125
(April 1, 1995)

We give equations and graphs for suggested variants of the current LIGO baffle configuration, and for the dominant scattered-light noise spectra for 4km interferometers in the LIGO beam tube: backscatter from baffles and diffraction off baffle edges. Throughout, we have tried to be as realistic as possible in our computations of scattered-light noise.

I. INTRODUCTION AND NOTATION

Building on our previous reports [1–3], we have computed with care the scattered-light noise for several variants of the candidate LIGO baffle configuration. Here we give only our final results; the derivations will be presented in a paper to be submitted to *Physical Review D*.

We have written a *Mathematica* Notebook [4] that computes numerically, from input parameters, the baffle locations and the scattering noise, based on the formulas given in this report. The numbers and graphs in this report were produced by that Notebook, and one can easily use the Notebook to explore the consequences of various changes in baffle parameters.

Our Notebook and this report use the same notation, much of which will be discussed in later sections:

- A_L — the amplitude transfer function from ground motion to *longitudinal* baffle motion (a function of frequency f), assuming normal-mode damping that is 0.02 of critical. This $A_L(f)$ is inferred from Mike Gamble's report [5].
- A_T — the amplitude transfer function from ground motion to *transverse* baffle motion assuming 0.02 damping; inferred from Gamble's report.
- f — gravity-wave frequency.
- H — maximum baffle height from tube wall to tips of highest serrations in the tube's transverse plane; assumed to be either 6cm or 8cm.
- dH — baffle safety factor [the baffles are treated as though they had height $H - dH$ (in the transverse plane) and no serrations, when computing the baffle separations that will just barely hide the beam wall from the most dangerous mirror]; dH is assumed to be 1cm.
- ΔH — mean depth of baffle serrations, peak to valley, in transverse plane; assumed to be 0.8cm.
- δH — amplitude of random variations of [average of the heights of adjacent baffle tips and valleys] in transverse plane; assumed to be 0.167cm.
- J_0 — the square of the amplification of backscatter noise due to off-centered mirrors; it is about 4 for main-beam axis 20 cm from the tops of the baffles [2].
- L — length of beam tube; 4km.
- l_n — distance from corner or end gate valve to baffle n; cf. Fig. 1.
- l_0, l_{oc}, l_{om}, l_{oe} — l_0 is the longitudinal distance from a gate valve to the center of the nearest test-mass chamber (the presumed location of a test-mass mirror for this report's modeling purposes); $l_{oc} = 12.4$m is the value of l_0 for the corner gate valve; $l_{om} = 5.7$m is for the mid-station gate valve; $l_{oe} = 7.8$m is for the end gate valve.
- $\bar{l}_0$ — the geometric mean of the distances from the corner and end gate valves to their nearest mirrors; $\bar{l}_0 = \sqrt{l_{oc} l_{oe}} = 9.8$ meters.
- N_B — number of baffles in one arm.
- N_Z — mean number of Fresnel zones subtended by a tooth of a serrated baffle.
- R — radius of beam tube.
- s_n — distance between baffle n and baffle $n+1$; cf. Fig. 1.
- W — transverse distance, from tube wall, of the farthest location, in the test-mass plane, at which the wall should be hidden by baffles; cf. Fig. 1. W is assumed to be 100cm.
- α — the coefficient appearing in the assumed law, $dP/d\Omega = \alpha/\theta^2$, for the mirrors' scattering probability; we set $\alpha = 10^{-6}$.
- β — the baffles' backscatter probability $\beta = dP/d\Omega$. For tube steel, $\beta \simeq 0.01$ to 0.02; for Martin black, $\beta \simeq 10^{-3}$; for black glass, $\beta \sim 10^{-5}$.
- β_n — fractional "reduced" distance of baffle n from the corner or end gate valve: $\beta_n = 4 l_n (L - l_n)/L$; it varies from 0 at the gate valves to unity at the tube's midpoint.
- λ — wavelength of the laser light.
- ρ — the fractional offset of the mirror centers and main-beam axis from the center of the tube; i.e. (distance of mirror centers from beam-tube axis)$/(R - H)$.
- ξ_s — the square root of the spectral density of ground displacement; assumed to be *twice* the LIGO site specification.

II. BAFFLE CONFIGURATION

A. Baffle Spacing

At the LIGO Baffle Review of 6&7 January 1995 it was agreed the baffle design should accomplish the following (cf. Sec. IV.2 of the Review minutes [6]):

1. Completely hide the entire beam-tube wall, beyond the gate valves, from the views of all test-mass mirrors.
2. Remove those baffles from the previous configuration that are not required to hide the beam tube.

3. Wherever possible, place the baffles at the fixed (not sliding) beam-tube supports.

In this report and our Notebook, we adopt a baffle configuration that accomplishes 1 and 3, but not 2. We have chosen to make the maximum separation between baffles be the same as the distance between fixed tube supports, 42m, so as to be sure of killing any stray light that scatters or diffracts into angles $\theta \lesssim 0.01$ and that thereby might travel from one end of the tube to the other with very few bounces and little attenuation. This is a simple safety factor that costs relatively little: an increase in the total number of baffles by about 30 out of roughly 1000 (3% increase) if the baffles are 6 inches high, and by about 65 out of rougly 750 (8% increase) if they are 8 inches high. (We are presently carrying out a Fokker-Planck analysis of forward propagation down the beam tube to determine whether this safety factor is really needed, and to firm up everyone's conviction that such forward propagating light will be so strongly attenuated that we do not need to worry about it.)

Our chosen baffle configuration, then, is the following:

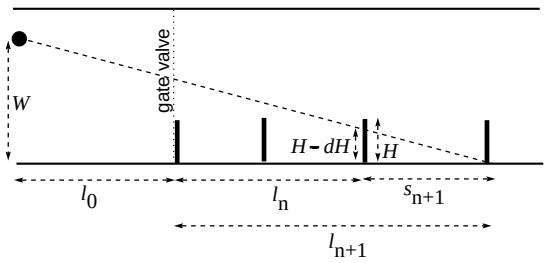

FIG. 1. Spacing of baffles near the ends of an interferometer.

Near each end of an interferometer (4km interferometer at both sites, and 2km interferometer at Hanford) the baffles have logarithmic spacings as shown in Fig. 1. The spacings are based on the viewpoint of a mirror that resides in the innermost test-mass chamber of the Phase C LIGO configuration, i.e. the chamber nearest the gate valve. The large dot in the figure is the most "extreme" point on such a mirror from which the tube wall must be hidden — i.e., the point whose distance W from the opposite wall is largest. In our numerical evaluations we use $W = 100$cm. The longitudinal distance l_0 from the test-mass mirror to the gate valve has the following values for the corner mirror at both sites (l_{0c}), the mid-station mirror at Hanford (l_{0m}), and the end mirror at both sites (l_{0e}):

$$l_{0c} = 12.4\text{m}, \quad l_{0m} = 5.7\text{m}, \quad l_{0e} = 7.8\text{m}. \tag{1}$$

The height of the highest tip on a serrated baffle in the transverse plane is H (6cm or 8cm in our evaluations), and the ray from the "extremal point" to the base of baffle $n+1$ passes through baffle n at a height $H - dH$. The "safety factor" dH (assumed 1cm in our evaluations) allows for serrations, tube sag, etc. Correspondingly, the distance s_{n+1} from baffle n to baffle $n+1$ is

$$s_{n+1} = (l_n + l_0)\left(\frac{H - dH}{W - H + dH}\right) \tag{2}$$

and the distance from the gate valve to baffle n is

$$l_n = l_0\left(\frac{W}{W - H + dH}\right)^n - l_0\ . \tag{3}$$

As one moves outward from the gate valve, the baffle spacing s_n increases. As soon as s_n grows larger than 42m, the baffle spacing is changed: thereafter the baffles are all placed at the tube's fixed-support locations, which are 42m apart.

In Tables 1, 2, 3, and 4, we list the locations (distances l_n) of the baffles at Hanford and at Livingston for $W =$ 100cm and $dH =$ 1cm and for baffle heights $H =$ 6cm and $H =$ 8cm. The total number of baffles (Hanford plus Livingston) is

$$\begin{aligned} N_{\text{total}} &= 614 + 458 = 1072 \text{ for 6 cm baffles} \\ &= 462 + 360 = 822 \text{ for 8 cm baffles.} \end{aligned} \tag{4}$$

Note that by increasing the baffle height from 6cm to 8cm we can reduce the number of baffles by 250 (about 25%). Note also that the presence of the midstation at Hanford increases the number of baffles there by about 30%. It turns out that the scattered-light noise is nearly independent of baffle height.

TABLE I. Locations of 6cm high baffles at Hanford. The numbers are the distances l_n of the baffles from the nearest corner or end gate valve, in centimeters.

65.	134.	206.	282.	363.
447.	536.	629.	727.	831.
940.	1055.	1176.	1303.	1437.
1577.	1726.	1882.	2046.	2219.
2401.	2593.	2794.	3007.	3230.
3466.	3713.	3974.	4248.	4537.
4841.	5161.	5498.	5853.	6226.
6619.	7033.	7468.	7926.	8409.
8917.	9451.	10014.	10606.	11230.
11886.	12577.	13304.	14070.	14875.
15724.	16616.	17556.	18545.	19587.
20683.	21837.	23051.	24330.	25676.
27092.	28583.	30153.	31805.	33545.
35375.	37303.	39331.	41466.	43714.
46080.	48571.	51192.	53952.	56857.
59914.	63133.	66521.	70087.	73842.
77793.	81953.	84000.	88200.	92400.
96600.	100800.	103400.	107600.	111800.
116000.	118026.	122153.	126074.	129799.
133337.	136699.	139893.	142926.	145809.
148547.	151148.	153619.	155967.	158197.
160315.	162328.	164240.	166057.	167782.
169422.	170979.	172459.	173864.	175200.
176468.	177673.	178818.	179906.	180939.

181920.	182853.	183739.	184580.	185380.
186139.	186861.	187546.	188197.	188816.
189404.	189962.	190492.	190996.	191475.
191930.	192362.	192772.	193162.	193533.
193884.	194219.	194536.	194838.	195125.
195397.	195655.	195901.	196135.	196356.
196567.	196767.	196957.	197138.	197310.
197473.	197627.	197775.	197914.	198047.
198173.	198293.	198407.	198515.	198618.
198715.	198808.	198896.	198980.	199059.
199135.	199207.	199275.	199340.	199401.
199460.	199515.	199568.	199618.	199666.
199711.	199754.	199795.	199833.	199870.
199905.	199938.	199970.	197400.	193200.
189000.	184800.	180600.	176400.	172200.
168000.	163800.	159600.	155400.	151200.
147000.	142800.	138600.	134400.	130200.
126000.	121800.	117600.	113400.	109200.
105000.	100800.	96600.	92400.	88200.
84000.	82252.	78101.	74157.	70410.
66850.	63469.	60256.	57204.	54305.
51551.	48934.	46449.	44087.	41844.
39713.	37688.	35765.	33937.	32202.
30552.	28986.	27498.	26084.	24741.
23464.	22252.	21101.	20007.	18967.
17980.	17042.	16151.	15304.	14500.
13736.	13010.	12321.	11666.	11043.
10452.	9891.	9357.	8850.	8369.
7911.	7477.	7064.	6672.	6299.
5945.	5609.	5289.	4986.	4698.
4424.	4164.	3916.	3682.	3459.
3247.	3045.	2854.	2672.	2500.
2336.	2180.	2032.	1891.	1758.
1631.	1510.	1396.	1287.	1184.
1085.	992.	904.	819.	739.
663.	591.	523.	458.	396.
337.	281.	228.	178.	130.
84.	41.			

TABLE II. Locations of 6cm high baffles at Livingston. The numbers are the distances l_n of the baffles from the nearest corner or end gate valve, in centimeters.

65.	134.	206.	282.	363.
447.	536.	629.	727.	831.
940.	1055.	1176.	1303.	1437.
1577.	1726.	1882.	2046.	2219.
2401.	2593.	2794.	3007.	3230.
3466.	3713.	3974.	4248.	4537.
4841.	5161.	5498.	5853.	6226.
6619.	7033.	7468.	7926.	8409.
8917.	9451.	10014.	10606.	11230.
11886.	12577.	13304.	14070.	14875.
15724.	16616.	17556.	18545.	19587.
20683.	21837.	23051.	24330.	25676.
27092.	28583.	30153.	31805.	33545.
35375.	37303.	39331.	41466.	43714.
46080.	48571.	51192.	53952.	56857.
59914.	63133.	66521.	70087.	73842.
77793.	81953.	84000.	88200.	92400.
96600.	100800.	105000.	109200.	113400.
117600.	121800.	126000.	130200.	134400.
138600.	142800.	147000.	151200.	155400.
159600.	163800.	168000.	172200.	176400.
180600.	184800.	189000.	193200.	197400.
197400.	193200.	189000.	184800.	180600.
176400.	172200.	168000.	163800.	159600.
155400.	151200.	147000.	142800.	138600.
134400.	130200.	126000.	121800.	117600.
113400.	109200.	105000.	100800.	96600.
92400.	88200.	84000.	82252.	78101.
74157.	70410.	66850.	63469.	60256.
57204.	54305.	51551.	48934.	46449.
44087.	41844.	39713.	37688.	35765.
33937.	32202.	30552.	28986.	27498.
26084.	24741.	23464.	22252.	21101.
20007.	18967.	17980.	17042.	16151.
15304.	14500.	13736.	13010.	12321.
11666.	11043.	10452.	9891.	9357.
8850.	8369.	7911.	7477.	7064.
6672.	6299.	5945.	5609.	5289.
4986.	4698.	4424.	4164.	3916.
3682.	3459.	3247.	3045.	2854.
2672.	2500.	2336.	2180.	2032.
1891.	1758.	1631.	1510.	1396.
1287.	1184.	1085.	992.	904.
819.	739.	663.	591.	523.
458.	396.	337.	281.	228.
178.	130.	84.	41.	

TABLE III. Locations of 8cm high baffles at Hanford. The numbers are the distances l_n of the baffles from the nearest corner or end gate valve, in centimeters.

93.	194.	302.	418.	542.
677.	821.	976.	1143.	1322.
1515.	1722.	1945.	2185.	2443.
2720.	3018.	3339.	3683.	4054.
4452.	4881.	5341.	5837.	6369.
6942.	7558.	8220.	8932.	9698.
10521.	11406.	12358.	13382.	14482.
15666.	16938.	18307.	19778.	21360.
23061.	24890.	26857.	28971.	31245.
33691.	36320.	39147.	42187.	45455.
48970.	52749.	56813.	58800.	63000.
67200.	71400.	75600.	79800.	84000.
88200.	92400.	96600.	100800.	103400.
107600.	111800.	116000.	120200.	124400.
128600.	132800.	137000.	141200.	141282.
145432.	149292.	152881.	156220.	159324.
162211.	164896.	167394.	169716.	171876.
173884.	175752.	177490.	179105.	180608.
182005.	183305.	184513.	185637.	186682.
187655.	188559.	189399.	190181.	190909.
191585.	192214.	192799.	193343.	193849.
194319.	194757.	195164.	195542.	195894.
196221.	196526.	196809.	197072.	197317.
197545.	197756.	197953.	198137.	198307.
198465.	198613.	198750.	198877.	198996.
199106.	199208.	199304.	199392.	199475.
199551.	199623.	199689.	199751.	199808.
199861.	199911.	199957.	197400.	193200.
189000.	184800.	180600.	176400.	172200.
168000.	163800.	159600.	155400.	151200.
147000.	142800.	138600.	134400.	130200.
126000.	121800.	117600.	113400.	109200.
105000.	100800.	96600.	92400.	88200.
84000.	79800.	75600.	71400.	67200.
63000.	58800.	55662.	51711.	48036.
44619.	41441.	38486.	35737.	33181.
30804.	28593.	26537.	24625.	22846.
21192.	19654.	18224.	16894.	15657.
14506.	13436.	12441.	11515.	10655.
9854.	9110.	8418.	7774.	7175.
6618.	6100.	5619.	5171.	4754.
4367.	4007.	3671.	3360.	3070.
2801.	2550.	2317.	2100.	1898.
1711.	1537.	1374.	1224.	1083.
953.	832.	719.	614.	516.
426.	341.	263.	190.	122.
59.7				

TABLE IV. Locations of 8cm high baffles at Livingston. The numbers are the distances l_n of the baffles from the nearest corner or end gate valve, in centimeters.

93.	194.	302.	418.	542.
677.	821.	976.	1143.	1322.
1515.	1722.	1945.	2185.	2443.
2720.	3018.	3339.	3683.	4054.
4452.	4881.	5341.	5837.	6369.
6942.	7558.	8220.	8932.	9698.
10521.	11406.	12358.	13382.	14482.
15666.	16938.	18307.	19778.	21360.
23061.	24890.	26857.	28971.	31245.
33691.	36320.	39147.	42187.	45455.
48970.	52749.	56813.	58800.	63000.
67200.	71400.	75600.	79800.	84000.
88200.	92400.	96600.	100800.	105000.
109200.	113400.	117600.	121800.	126000.
130200.	134400.	138600.	142800.	147000.
151200.	155400.	159600.	163800.	168000.
172200.	176400.	180600.	184800.	189000.
193200.	197400.	197400.	193200.	189000.
184800.	180600.	176400.	172200.	168000.
163800.	159600.	155400.	151200.	147000.
142800.	138600.	134400.	130200.	126000.
121800.	117600.	113400.	109200.	105000.
100800.	96600.	92400.	88200.	84000.
79800.	75600.	71400.	67200.	63000.
58800.	55662.	51711.	48036.	44619.
41441.	38486.	35737.	33181.	30804.
28593.	26537.	24625.	22846.	21192.
19654.	18224.	16894.	15657.	14506.
13436.	12441.	11515.	10655.	9854.
9110.	8418.	7774.	7175.	6618.
6100.	5619.	5171.	4754.	4367.
4007.	3671.	3360.	3070.	2801.
2550.	2317.	2100.	1898.	1711.
1537.	1374.	1224.	1083.	953.
832.	719.	614.	516.	426.
341.	263.	190.	122.	59

B. Baffle Serrations

The baffles must be serrated to control noise due to diffraction of scattered light off the baffle edges; see Fig. 2. The serrations accomplish two things:

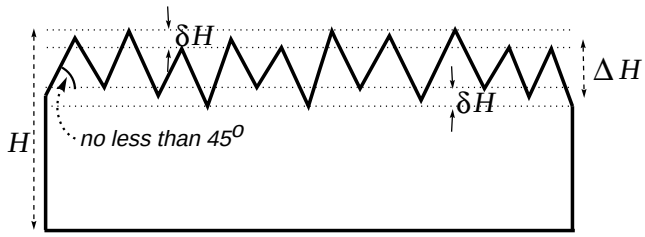

FIG. 2. Baffle serrations, projected onto the beam tube's transverse plane.

First: Each serration tooth averages the scattered light over as many Fresnel zones as it intercepts, thereby reducing substantially the diffracted-light noise. We have not yet solved the problem of what tooth shape maximizes the noise reduction, but we know that a simple sawtooth does quite well, so for now we recommend that the tooth shape be a saw-tooth (inverted V). To get the full noise reduction, the slope of the V's edges to the beam-pipe wall should be no less than 45^o. (This minimum was deduced for 0.4cm deep serrations. At Whitcomb's urging we have deepended them to 0.8 cm, and correspondingly we might have to steepen the 45^o minimum angle.) For a sawtooth shape, the amplitude noise reduction factor, rms averaged over serrations, is

$$\mathcal{R}_{\rm sawtooth} = \frac{\sqrt{2}}{\pi N_Z} = \frac{\sqrt{2}\lambda L}{8\pi(R-H)\Delta H}\ , \qquad (5)$$

where N_Z is the mean number of Fresnel zones subtended by the teeth, from peak to valley, and where the second expression is for a main beam centered in the beam tube and baffles at the tube's midpoint. We recommend that the mean peak-to-valley serration depth projected onto the transverse plane, ΔH, be as large as is compatible with other constraints; we have chosen 0.8cm, giving $\mathcal{R}_{\rm sawtooth} \simeq 1/40$ for centered beam, tube midpoint, and green light. (We are a little unsure as to whether the full 1/40 noise reduction can actually be achieved; it might require too great a precision in baffle machining. We plan to explore the allowed tolerances.)

Second: The heights of the serration peaks and valleys should be randomized so as to ensure that phase coherence is broken around each baffle and from one baffle to the next. The following principles should be followed in this randomization:

1. The average of the peak-to-valley height along a tooth edge, projected into the transverse plane, should vary randomly by an amount $\delta H =$ 0.167cm, with a uniform probability distribution $dP/d\text{height} = 1/\delta H$. The total variation $\delta H =$ 0.167cm is two Fresnel zones of thickness (2π phase variation) for 1.03μm light at the tube's midpoint, when the main beam is centered in the tube. The half-widths of the teeth, peak to valley, should all be the same despite the varying peak-to-valley height. [If one prefers to hold fixed the angles of the tooth edges to the radial direction, so the tooth half-width is proportional to the peak-to-valley height, then one must use a probability distribution $dP/d\text{height} \propto 1/(\text{peak-to-valley height})$ over the range $\Delta H - \delta H$ to $\Delta H + \delta H$.]

2. The lateral coherence length (coherence length along the baffle's rim) for these tooth-height variations should be no larger than $\sim \sqrt{\lambda_{\rm green} L/4} \simeq$ 2cm (the minimum size over which incoherence can be produced in the face of beam spreading between the mirrors and baffles at the tube's midpoint).

3. The baffles can be identical, with the same random pattern of serration heights; but if they are identical, then successive baffles should be rotated randomly relative to each other in the tube.

These principles should guarantee that phase coherence is broken to the maximum extent possible; cf. Eq. (9).

C. Baffle Helicity and Inclination

Each baffle should be wound around the tube's circumference in a helical way, and its face should be inclined away from the nearest test-mass mirror in the manner of the original baffle design. It is important that this inclination and helicity be chosen in such a way that

- the only regions of any baffle which can reflect light specularly from one test-mass mirror to the other, or from a mirror back to itself, are tiny spots; there must be no reflecting curves or surfaces.

III. BAFFLE VIBRATIONS

Mike Gamble [5] has computed the amplitude transfer functions from ground motion to beam-tube motion at representative locations on the beam tube. As we understand it, Gamble assumes that the fixed tube supports and the sliding tube supports are driven by ground motions with the following properties:

1. The spectral densities of this ground displacement $\tilde{\xi}_g^2(f)$ are identically the same in all three directions (longitudinal, horizontal-transverse, and vertical) and are the same at all supports.

2. The cross correlation spectra of the ground displacements in the three directions and at the various supports all vanish.

Gamble picks three horizontal locations along the beam tube: one 1/4 of the way from a fixed support to a sliding support (the "1/4-point"), one 1/2 way from fixed to sliding support (the "1/2-point"), and one on the sliding support (the "1-point"). As we understand it, Gamble computes at each of these points the spectral density of the tube displacement, $\tilde{\xi}_t^2(f)$ in the three orthogonal directions; and he then computes the ratio of this tube-displacement spectral density to the ground-displacement spectral density

$$A^2(f) = \frac{\tilde{\xi}_t^2(f)}{\tilde{\xi}_g^2(f)} \tag{6}$$

for each of the three orthogonal directions. He denotes this "transfer function" A_x^2 for tube displacement in the longitudinal direction, A_y^2 for tube displacement in the vertical direction, and A_z^2 for tube displacement in the horizontal-transverse direction.

Gamble computes these transfer functions using three different models: a shell model (which takes account of the tube's thin-shell structure and dynamics) with all normal modes damped at a rate 4% of critical damping; a beam model (which treats the tube as a beam that has no internal dynamics) with 4% damping; and a beam model with 2% damping. Gamble gives plots of $A_x^2(f)$, $A_y^2(f)$, and $A_z^2(f)$ for these three models and for the three points on the tube. (For the shell model, as we understand it, he chooses each point at an azimuth around the tube where the spectral peaks are particularly high; i.e., he puts his point near the maxima of the modal eigenfunctions.) In Table 1 of his report, Gamble summarizes some features of the most strongly excited normal modes. Note that in this table he lists the values of the *amplitude* transfer function A on resonance for the location and direction where it is greatest; in his figures, he shows the *power* transfer functions $A^2(f)$.

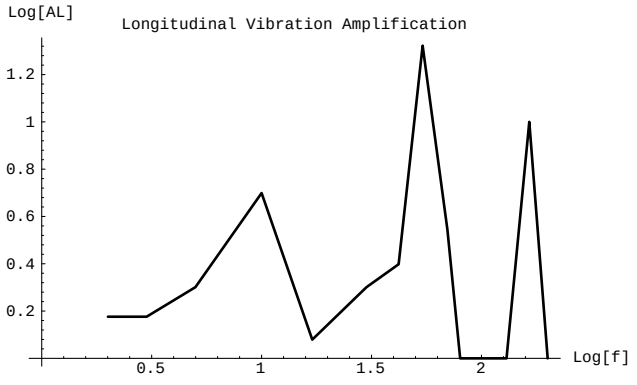

FIG. 3. The longitudinal amplitude transfer function A_L from ground displacement to beam-tube displacement, rms averaged over the beam tube. Plotted horizontally is $\log_{10} f$ with frequency f in Hz; plotted vertically is $\log_{10} A_L$.

We have used Gamble's figures and table to construct a longitudinal amplitude transfer function $A_L(f)$ and a transverse amplitude transfer functon $A_T(f)$ for use in evaluating scattered-light noise.

The $A_L(f)$ [shown in Fig. 3] is our estimate of the longitudinal amplification factor with damping 2% of critical, rms-averaged over the beam tube's interior. We computed this $A_L(f)$ by taking Gamble's amplitude amplification spectra $A_x(f)$ and rms averaging them over the 1-point, 1/2-point, 1/4-point, a 0-point (the fixed support location, where we assumed $A_x = 1$), and an extrapolated 3/4-point. In this computation we always used the largest amplification factor from Gamble's three models, and for his 0.04-loss models, on and near resonance we multiplied by a factor 2 to correct to an 0.02 loss. We have used a far more coarse frequency grid than did Gamble, always making sure that the grid includes the peaks of the largest resonances; the coarseness of our grid artificially broadens the resonances, but it correctly depicts the resonance peaks and the bottoms of the valleys between resonances.

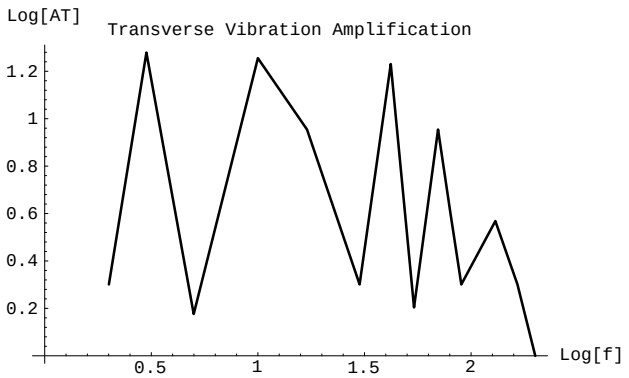

FIG. 4. The transverse amplitude transfer function A_T from ground displacement to beam-tube displacement, rms averaged over the tube. Plotted horizontally is $\log_{10} f$ with frequency f in Hz; plotted vertically is $\log_{10} A_T$.

Our tranverse amplitude transfer function $A_T(f)$ [shown in Fig. 4] is the amplitude amplification, rms averaged over the beam tube and over the vertical direction and horizontal-transverse direction. We computed it from Gamble's figures and table by the same procedure as for $A_L(f)$, except that in addition to the rms averaging described for A_L, we also rms averaged over A_y and A_z.

Notice that the highest resonances of $A_L(f)$ and $A_T(f)$ represent 20-fold rms amplifications of the ground's amplitude motion; this corresponds to a *peak* power amplification of 1000 as shown in Gamble's figures, which gets reduced to 1000/2 when averaged over the beam tube, and then gets further reduced to $\sqrt{1000/2} \simeq 20$ when converted from an average power to an rms average amplitude. The most troublesome resonance, as we shall see, is that of the longitudinal mode at 52 Hz; it rep-

resents a stretching of the tube between fixed supports. Also of concern, as we shall see, are the longitudinal and transverse resonances near 10Hz.

In our noise computations, we assumed that the amplitude spectrum of ground motions $\tilde{\xi}_g(f)$ is twice the LIGO site-specification; see Fig. 5. We included the factor two because the backscatter noise is strongly influenced by baffles near the gate valves, where cultural activity may well double the ground motion—and also because wind may significantly enhance it.

We assume that the baffles' displacement spectrum is $A_L(f)\tilde{\xi}_g(f)$ in the longitudinal direction, and $A_T(f)\tilde{\xi}_g(f)$ in transverse directions; i.e., we assume that the baffles themselves do not dynamically amplify the tube's motion.

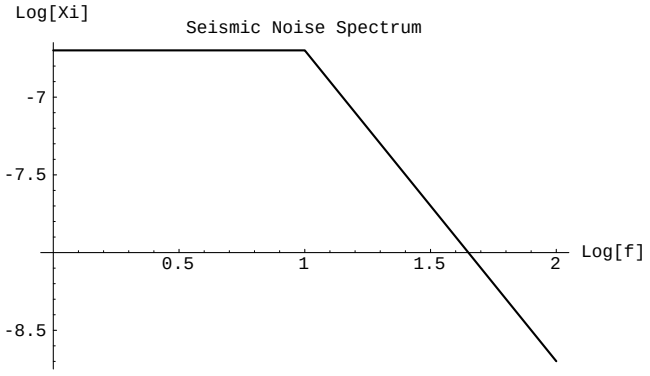

FIG. 5. Our assumed amplitude spectrum of ground motion, $\tilde{\xi}_g(f)$; this is twice the noise level for the LIGO site specification. Plotted horizontally is $\log_{10} f$ with frequency f in Hz; plotted vertically is $\log_{10} \tilde{\xi}_g$ with $\tilde{\xi}_g$ in units cm/$\sqrt{\text{Hz}}$.

IV. STANDARD QUANTUM LIMIT

The standard quantum limit for a one ton test mass is

$$\tilde{h}_{\rm SQL} = \left(\frac{8\hbar}{m(2\pi f L)^2}\right)^{1/2} = \frac{4\times 10^{-24}}{\sqrt{\rm Hz}}\left(\frac{10{\rm Hz}}{f}\right) . \quad (7)$$

The goal agreed upon at the 6&7 January Baffle Review is to try to keep the scattered-light noise below 1/10 this standard quantum limit.

V. BACKSCATTER NOISE

The noise due to backscatter off baffles is given by the following formula:

$$\tilde{h}_{\rm BS} = \frac{\alpha\lambda A_L \xi_s}{RL}\sqrt{4\pi\beta\ln(L/l_0)J_0}\,; \quad (8)$$

cf. Eq. (1) of Ref. [2]. The factor $\ln(L/l_0)$ comes from integrating over the entire length of the tube, from the gate valve's location a distance l_0 beyond the test-mass mirror, to the distant end of the tube a distance L away. The factor β is the baffles' backscatter probability $\beta = dP/d\Omega$, which has the values

- $\beta \simeq 0.01$ to 0.02 for beam-tube steel.
- $\beta \simeq 10^{-3}$ for Martin black.
- $\beta \sim 10^{-5}$ for black glass.

Figure 6 shows the backscatter noise (8) for each of these materials, with green light; and Fig. 7 shows it with 1.03μm light. For comparison we also show the standard quantum limit (7).

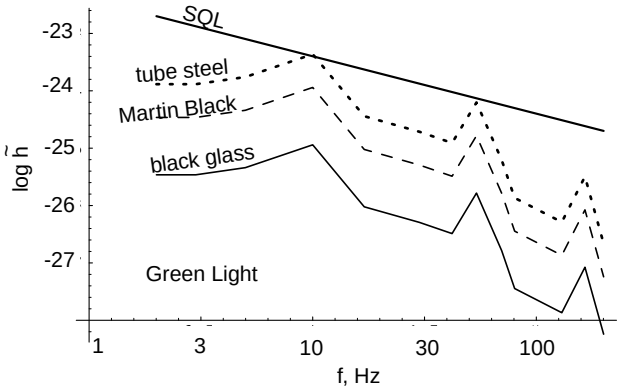

FIG. 6. Backscatter noise for green light and for three different baffle materials.

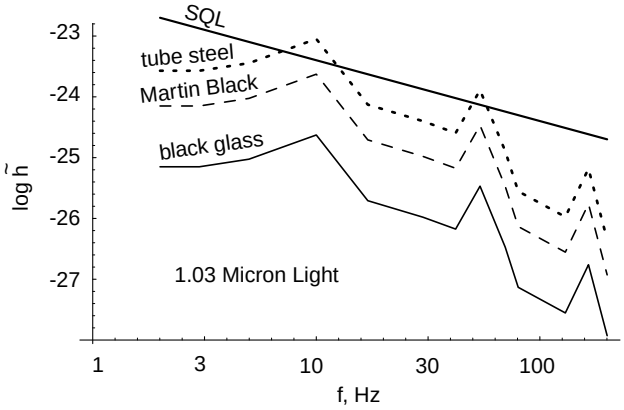

FIG. 7. Backscatter noise for 1.03μm light and for three different baffle materials.

Notice that the beam-tube steel has noise about twice the standard quantum limit (2×SQL) at the troublesome resonances and about SQL/3 in the broad valley between $\sim$ 20 and $\sim$ 50 Hz (a crucial region), when 1.03μm light is used; and for green light, it is at the SQL on resonance. By contrast, Martin black (or any other "Martin-black-like" material with backscatter $\beta \simeq 10^{-3}$) is about SQL/2 on resonance at 1.02μm and meets the SQL/10 goal everywhere off resonance at either wavelength, 1.03μm or green.

VI. DIFFRACTION NOISE FOR CENTERED MIRRORS

When the mirrors and main beam are centered in the beam tube, noise due to diffraction of scattered light off the baffles is given by the following formula:

$$\tilde{h}_{\rm Diff,Cen} = \left(\frac{\alpha\lambda A_T \xi_s \sqrt{N_B}}{(R-H)L}\right)\left(\frac{\sqrt{2}\lambda L}{8\pi(R-H)\Delta H}\right) \times \left[\frac{\sqrt{\lambda L/4}}{2\pi(R-H)}\right]^{1/2}\left[\frac{1}{N_B}\sum_{n=1}^{N_B}\beta_n^2\right]^{1/2} . \quad (9)$$

The various terms in this equation have the following physical origins:

1. The first term is the diffraction noise for centered mirrors in the absence of any baffle serration and with perfect coherence around each baffle, but perfect incoherence from one baffle to the next, and with all N_B baffles idealized as contributing equally.

2. The second term is the noise reduction due to each serration tooth subtending (and thus averaging over) several Fresnel zones; cf. Eq. (5) For our choice of deep serrations, $\Delta H = 0.8cm$, this reduction factor is about 1/40 in the green and 1/20 at 1.03μn. (Recall that we are a bit worried over whether the full 1/40 reduction can be achieved because of baffle tolerances, and we plan to explore this.)

3. The third term is the noise reduction due to breaking phase coherence around the baffles.

4. The fourth term produces the proper weighting of the baffles (including the dependence of the noise reduction factors on their locations). In this fourth term $\beta_n = 4l_n(L-l_n)/L^2$ is the "reduced fractional distance" of baffle n from the mirrors; it varies from zero at the tube ends to unity at the tube midpoint. The values of this fourth term for the Hanford and Livingston sites, with green light, are 0.65 and 0.49. The ratio $0.65/0.49 = 1.33$ multiplied by the ratio of the square root of the number of baffles, $\sqrt{614/458} = 1.16$, represents a 50% increase in diffraction noise for 4km interferometers, produced by the large set of baffles near the Hanford midstation. For 1.054 micron light the numbers are similar.

We will graph this diffraction noise for centered mirrors in the next section, along with that for off-center mirrors.

VII. DIFFRACTION NOISE FOR OFF-CENTER MIRRORS

For mirrors offset by a distance $\rho(R-H) \gg \sqrt{\lambda L/4} \sim$ 2cm from the beam tube's central axis, the diffraction noise has the following form:

$$\tilde{h}_{\rm Diff,OC} = \left(\frac{\alpha\lambda A_T \xi_s \sqrt{N_B}}{(R-H)L}\right)\left(\frac{\sqrt{2}\lambda L}{8\pi(R-H)\Delta H}\right) \times \left(\frac{\sqrt{\lambda L/4}}{2\pi(R-H)}\right)\left[\frac{1}{N_B}\sum_{n=1}^{N_B}\beta_n^3\right]^{1/2} G(\rho) , \quad (10)$$

where

$$G(\rho) = \left[\frac{1}{\rho}\left(\frac{1}{(1-\rho)^6}+\frac{1}{(1+\rho)^6}\right)\right]^{1/2} = \frac{\sqrt{2(1+15\rho^2+15\rho^4+\rho^6)}}{\sqrt{\rho}(1-\rho^2)^3} . \quad (11)$$

The various terms in $\tilde{h}_{\rm Diff,OC}$ [Eq. (10)] have the following origins:

1. The first term is the noise for a centered mirror and unserrated baffles with perfect coherence around each baffle but incoherence from baffle to baffle—and with all baffles weighted equally.

2. The second term is the noise reduction due to each baffle tooth's averaging over several Fresnel zones [cf. Eq. (5)]. This second term was not present in our previous report [3] because when we wrote that report, we mistakenly suspected that off-centering the beam would prevent this reduction factor from occuring. We are now convinced that, for sufficiently carefully designed serrations, this reduction can be achieved both off-center and on, and both with our specified type of randomness and with no randomness at all. For centered mirrors (previous section), we worry about achieving the full reduction implied by this second term; for off-centered mirrors we worry much less because the reduction is more modest by a factor $1/(1-\rho) \simeq 3$ (which is included in the function $G(\rho)$ described below).

3. The third term is the noise reduction due to breaking of coherence produced by the pattern of Fresnel zones along the mean baffle edge. Note that this coherence-breaking term is the square of the one for centered baffles, i.e. the coherence breaking is much more effective in this off-centered case than for centered beams. The reason is that here coherence is broken by the baffle edges' cutting the beam's Fresnel-zone pattern, whereas for centered beams it is broken by incoherent irregularities in the mirrors and the baffle serrations. The cutting of the Fresnel-zone pattern is more effective than the irregularities.

4. The fourth term produces the proper weighting of baffles. Note that the weighting is β_n^3 here but β_n^2 for centered baffles. For Hanford and Livingston with 6cm baffles and green light, this last term is 0.63 and 0.44. The ratio $0.63/0.44 = 1.43$ multiplied by the square root of the number of baffles at the two sites $\sqrt{614/458} = 1.16$ represents a 65% noise increase due to the many baffles near the mid-station at Hanford.

5. The last term, $G(\rho)$, corrects for the off-centering of the mirrors. Notice that for substantially off-set mirrors, $G(\rho) \simeq 1/(1-\rho)^3 \simeq$ [(tube radius)/(distance of main beam from tops of nearest baffles)]^3. This is a sharper dependence on distance to the baffles than we have reported before [3], because we previously were not using deep serrations to reduce the diffraction noise for off-centered mirrors (cf. discussion of second term above).

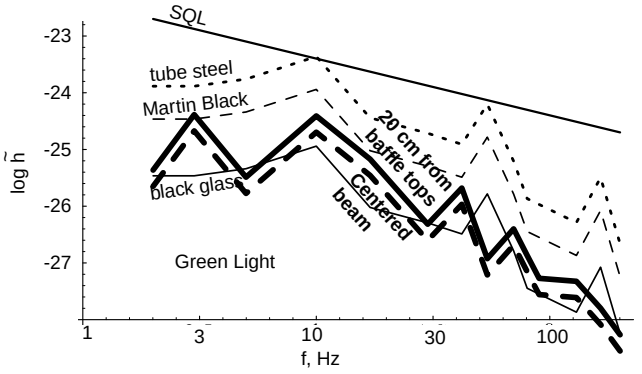

FIG. 8. Diffraction noise (thick curves) for green light, compared to backscatter noise (thin curves), at Hanford with 6cm high baffles and 0.8cm deep serrations. The thick solid curve is for the main-beam axis 20cm away from the nearest baffle tops; the thick dashed curve is for the main-beam axis at the center of the beam tube. The scattering noise is the same as shown in Fig. 6

The thick solid curve in Figure 8 depicts this off-center diffraction noise, for a green main beam that is 20cm from the tops of the baffles ($\rho = 0.63$) at Hanford, and for 6cm high baffles. The noise is not very sensitive to the baffle height, but it is quite sensitive to the wavelength of the light $\tilde{h}_{\rm DIFF,OC} \propto \lambda^3$; for 1.03micron light (Fig. 9) the off-center diffraction noise is 9 times worse than for green.

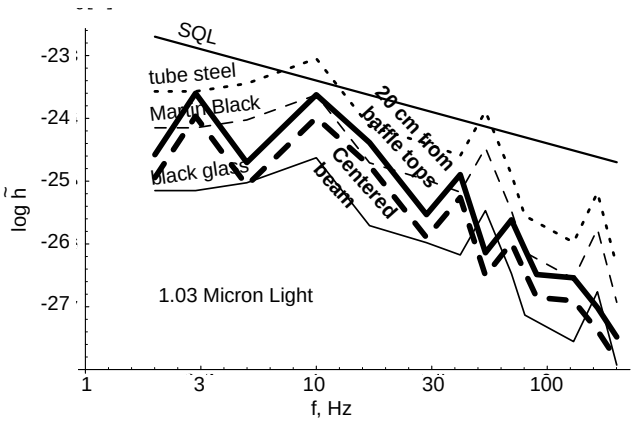

FIG. 9. Diffraction noise (thick curves) for 1.03 micron light, compared to backscatter noise (thin curves), at Hanford with 6cm high baffles and 0.8cm deep serrations. The thick solid curve is for the main-beam axis 20cm away from the nearest baffle tops; the thick dashed curve is for the main-beam axis at the center of the beam tube. The scattering noise is the same as shown in Fig. 7

Figures 8 and 9 compare the off-center diffraction noise (thick solid curve) with diffraction noise for centered beams (thick dashed curves). There is not a great difference: For the main-beam axis 20cm from the baffle tops ($\rho = 0.63$), the $G(\rho)$ factor worsens the noise by a factor 24; but this same off-centering of the beam improves the coherence breaking by a factor $[\sqrt{\lambda L/4}/2\pi(R-H)]^{1/2} \simeq 1/12$; so the net noise worsening is only a factor 2.

Figures 8 and 9 also compare the diffraction noise (thick curves) with backscatter noise (thin curves). Notice that the diffraction noise is sufficiently large to swamp the backscatter noise from black-glass baffles, but it is generally less than or of order backscatter for Martin-black-like materials. This suggests that we should aspire to achieve a backscatter that is like that of Martin black, or a little better; but there is *not* a strong motivation, on the basis of noise, to push well beyond $\beta \sim 10^{-3}$ toward black glass's $\beta \sim 10^{-5}$.

The large diffraction noise at the 10Hz resonance ($\simeq$SQL for 1.03μm) is disappointing, and we don't know a practical way to reduce it (aside from improving the mirrors to $\alpha < 10^{-6}$). However, away from that resonance, the diffraction noise is generally well within our goal of 0.1SQL.

[1] K. S. Thorne, "Light Scattering and Proposed Baffle Configuration for the LIGO," LIGO technical report and Caltech Theoretical Astrophysics Preprint GRP-200, Febru-

ary 1989.

[2] E. E. Flanagan and K. S. Thorne, "Noise due to backscatter off baffles, the nearby wall, and objects at the far end of the beam tube; and recommended actions," LIGO technical report, 2 August 1994.

[3] E. E. Flanagan and K. S. Thorne, "Light Scattering and Baffle Configuration for LIGO," Report prepared for LIGO baffle review, 6&7 January 1995.

[4] E. E. Flanagan and K. S. Thorne, "Evaluation of Scattered-Light Noise for LIGO" a Mathematica Notebook, 2 April 1995.

[5] M. Gamble, "LIGO Beam Tube Study Report (Dynamic Response of the Beam Tube to the Hanford, WA Site Ambient Vibration Spectrum)", LIGO-T950005-00-D, 7 March 1995.

[6] K. S. Thorne, *Minutes of Review of LIGO Baffle Design and Light Scattering in the Beam Tube*, 6&7 January 1995.